# Automatic Signal Extraction for Stationary and Non-Stationary Time Series by Circulant SSA

Bógalo, Juan and Poncela, Pilar and Senra, Eva

Universidad de Alcalá, European Commission, Joint Research Centre (JRC), Universidad de Alcalá

5 January 2017

# Automatic Signal Extraction for Stationary and Non-Stationary Time Series by Circulant SSA*

Juan Bógalo
Universidad de Alcalá
SPAIN

Pilar Poncela
European Commission, Joint Research Centre (JRC)
ITALY

Eva Senra
Universidad de Alcalá
SPAIN

January 5, 2017

**Abstract**

Singular Spectrum Analysis (SSA) is a nonparametric tecnique for signal extraction in time series based on principal components. However, it requires the intervention of the analyst to identify the frequencies associated to the extracted principal components. We propose a new variant of SSA, Circulant SSA (CSSA) that automatically makes this association. We also prove the validity of CSSA for the nonstationary case. Through several sets of simulations, we show the good properties of our approach: it is reliable, fast, automatic and produces strongly separable elementary components by frequency. Finally, we apply Circulant SSA to the Industrial Production Index of six countries. We use it to deseasonalize the series and to illustrate that it also reproduces a cycle in accordance to the dated recessions from the OECD.

**Keywords**: circulant matrices, signal extraction, singular spectrum analysis, nonparametric, time series, Toeplitz matrices.

**JEL Classification**: C22, E32

*The views expressed in this paper are those of the authors and should not be attributed to the European Commission. First and third authors acknowledge financial support from the Spanish government, contract grants ECO2015-70331-C2-1-R, ECO2014-56676C2-2-P and ECO2015-66593-P.

# 1 Introduction

In many occasions, macroeconomic policy relies on analyzing a particular signal from the observed time series as the cycle or the trend. Additionally, statistical offices need to produce seasonally adjusted data for a large amount of economic indicators. Singular Spectrum Analysis (SSA) is a non-parametric (and, therefore, model free) procedure based on subspace algorithms for signal extraction. The main task in SSA is to extract the underlying components of a time series like the trend, cycle, seasonal and irregular components. It has been applied to a wide range of time series problems, besides signal extraction, like forecasting, missing value imputation and others. SSA builds a trajectory matrix by putting together lagged pieces of the original time series and works with the Singular Value Decomposition of this matrix. It is a procedure closely related to Principal Component (PC) analysis but applied to the trajectory matrix.

SSA has been applied in several fields. In economics, Hassani and Thomakos (2010) review SSA for economic and financial time series, focusing on forecasting and the business cycle monitoring. Regarding forecasting, Hassani, Heravi, Brown and Ayoubkani (2013) and Silva and Hassani (2015) focus on the effects of forecasting with SSA before and after the 2008 recession, Hassani, Soofi and Zhigljavsky (2013) forecast the inflation dynamics or Hassani, Heravi and Zhigljavsky (2013) forecast industrial production with multivariate SSA. Related to business cycles, de Carvalho, Rodrigues and Rua (2012) track the US business cycle, de Carvalho and Rua (2017) focus on the real time nowcasting of the output gap and Sella, Vivaldo, Groth and Ghil (2016) analyze economic cycles and their synchronization in three European countries. SSA has also been applied to estimate stochastic volatility models by Arteche and García-Enríquez (2016).

However, an important drawback of the initial SSA procedures is that the intervention of the analyst is required to identify the harmonic frequencies of the extracted components. To solve this problem we propose a new SSA methodology based on circulant matrices (CSSA). The main feature of these matrices is that their eigenstructure can be obtained as a function of the frequencies and therefore we can automatically identify the eigenvalues and eigenvectors associated to any particular frequency. Moreover, we also prove the validity of our proposal for nonstationary time series as well. An additional contribution of our method is the strong separability of the extracted components as compared to previous variants of SSA.

In summary, our contribution is to propose Circulant SSA to automatically apply SSA

for signal extraction, without the intervention of the analyst, recovering reliable components that are strongly separable for both stationary and nonstationary time series.

The structure of this paper is as follows: Section 2 briefly describes the SSA technique. Section 3 proposes our new SSA procedure, named after Circulant SSA and proves its use for nonstationary time series too. Section 4 verifies the strong separability of the extracted components. Section 5 presents a set of simulations to check the properties of the proposed methodology and Section 6 applies it to several real time series. Finally, Section 7 concludes.

## 2 SSA methodology

The origin of SSA dates back to 1986 with the publication of the papers by Broomhead and King (1986a, 1986b) and Fraedrich (1986). Vautard and Ghil (1989) introduce Toeplitz SSA under the assumption of stationary time series and Vautard et al. (1992) further develop the technique and are the first to derive an algorithm to obtain the extracted components with the length of the original series. At the same time, and independently, the so-called Caterpillar technique was developed in the former Soviet Union (see, Danilov and Zhigljavsky, 1997). Elsner and Tsonis (1996), Golyandina et al. (2001) and Golyandina and Zhigljavsky (2013) are books on the topic.

In this section we briefly describe the steps of the SSA technique to decompose a time series in its unobserved components. Let $\{x_t\}$ be a real valued time series of size $T$, $\mathbf{x} = (x_1, ..., x_T)'$, and $L$ a positive integer, called the window length, such that $1 < L < T/2$. The Basic SSA or Broomhead-King (BK) procedure involves 4 steps:

**1st step: Embedding**

From the original time series we will obtain an $L \times N$ trajectory matrix $\mathbf{X}$ given by $L$ dimensional time series of length $N = T - L + 1$ as

$$\mathbf{X} = (\mathbf{x}_1|...|\mathbf{x}_N) = \begin{pmatrix} x_1 & x_2 & x_3 & ... & x_N \\ x_2 & x_3 & x_4 & ... & x_{N+1} \\ \vdots & \vdots & \vdots & \vdots & \vdots \\ x_L & x_{L+1} & x_{L+2} & ... & x_T \end{pmatrix}$$

where $\mathbf{x}_j = (x_j, ..., x_{j+L-1})'$ indicates the vector of dimension $L$ and origin at time $j$. Notice that the trajectory matrix $\mathbf{X}$ is Hankel and both, by columns and rows, we obtain subseries of the original one.

**2nd step: Decomposition**

In this step, we perform the singular value decomposition (SVD) of the trajectory matrix $\mathbf{X} = \mathbf{U}\mathbf{D}^{1/2}\mathbf{V}'$ where $\mathbf{U}$ is the $L \times L$ matrix whose columns $\mathbf{u}_k$ are the eigenvectors of the second moment matrix $\mathbf{S} = \mathbf{X}\mathbf{X}'$, $\mathbf{D} = diag(\tau_1, ..., \tau_L)$, $\tau_1 \geq ... \geq \tau_L \geq 0$, are the eigenvalues of $\mathbf{S}$ and $\mathbf{V}$ is the $N \times L$ matrix whose columns $\mathbf{v}_k$ are the $L$ eigenvectors of $\mathbf{X}'\mathbf{X}$ associated to nonzero eigenvalues. This decomposition allows to write $\mathbf{X}$ as the sum of the so-called elementary matrices $\mathbf{X}_k$ of rank 1,

$$\mathbf{X} = \sum_{k=1}^{r} \mathbf{X}_k = \sum_{k=1}^{r} \mathbf{u}_k \mathbf{w}_k',$$

where $\mathbf{w}_k = \mathbf{X}'\mathbf{u}_k = \sqrt{\tau_k}\mathbf{v}_k$ and $r = \max_{\tau_k > 0}\{k\}$=rank($\mathbf{X}$).

**3rd step: Grouping**

Under the assumption of weak separability given in Golyandina et al. (2001), we group the elementary matrices $\mathbf{X}_k$ into $m$ disjoint groups summing up the matrices within each group. Let $I_j = \{j_1, ..., j_p\}, j = 1, ..., m$ each disjoint group of indexes associated to the corresponding eigenvectors. The matrix $\mathbf{X}_{I_j} = \mathbf{X}_{j_1} + ... + \mathbf{X}_{j_p}$ is associated to the $I_j$ group. The decomposition of the trajectory matrix into this groups is given by $\mathbf{X} = \mathbf{X}_{I_j} + ... + \mathbf{X}_{I_m}$. The contribution of the component coming from matrix $\mathbf{X}_{I_j}$ is given by $\sum_{k \in I_j} \tau_k / \sum_{k=1}^{r} \tau_k$.

**4th step: Reconstruction**

Let $\mathbf{X}_{I_j} = (\widetilde{x}_{ij})$. In this step, each matrix $\mathbf{X}_{I_j}$ is transformed into a new time series of the same length $T$ as the original one, denoted as $\widetilde{\mathbf{x}}^{(j)} = (\widetilde{x}_1^{(j)}, ..., \widetilde{x}_T^{(j)})'$ by diagonal averaging of the elements of $\mathbf{X}_{I_j}$ over its antidiagonals as follows

$$\widetilde{x}_t^{(j)} = \left\{ \begin{array}{ll} \frac{1}{t}\sum_{i=1}^{t} \widetilde{x}_{i,t-i+1}, & 1 \leq t < L \\ \frac{1}{L}\sum_{i=1}^{L} \widetilde{x}_{i,t-i+1}, & L \leq t \leq N \\ \frac{1}{T-t+1}\sum_{i=L-N+1}^{T-N+1} \widetilde{x}_{i,t-i+1}, & N < t \leq T \end{array} \right\}.$$

The alternative Toeplitz SSA or Vautard-Ghil (VG) relies on the assumption that $\mathbf{x}$ is stationary and zero mean and it performs the SVD decomposition in step 2 from an alternative matrix $\mathbf{S}_T$= $(s_{ij})$ where

$$s_{ij} = \frac{1}{T - |i-j|} \sum_{m=1}^{T-|i-j|} x_m x_{m-|i-j|}, \qquad 1 \leq i, j \leq L. \tag{1}$$

In this case, the matrix $\mathbf{S}_T$ is the sample lagged variance-covariance matrix of the original series, a symmetric Toeplitz matrix. The set $(\tau_k, \mathbf{u}_k, \mathbf{w}_k)$ is named the $k$-th eigentriple. The rest of the algorithm remains unchanged.

# 3 Circulant SSA

As previously stated in the introduction, a drawback of SSA in any of its variants is that it requires the intervention of the analyst to identify the harmonic frequencies of the extracted components. To try to overcome this problem, Ghil and Mo (1991), associate two different extracted principal components with similar eigenvalues to the same oscillation if they are highly correlated for a given lag. Vautard et al. (1992) suggest a test based on the periodogram to establish if a pair of eigenvectors are associated to the same harmonic. Later, Alexandrov and Golyandina (2004, 2005) introduce optimal thresholds for grouping eigenvectors linked to nearby frequencies in order to assign them to the same harmonic. Alonso and Salgado (2008) and Bilancia and Campobasso (2010) apply cluster techniques for grouping the elementary components based on k-means and hierarchical clustering, respectively. Nevertheless, whatever procedure is used, the grouping of frequencies is made after the elementary components are extracted. Also, the previous tests and procedures are based on parameters and/or thresholds that have to be previously set in a subjective way. Since the pairs of eigenvalues and eigenvectors are obtained, not as a function of the frequency, but rather on a decreasing magnitude, this means that the grouping is done with uncertainty. Bozzo et al. (2010) provided a partial solution by linking the eigenvalues-eigenvectors as a function of the frequency for symmetric positive definite Toeplitz matrices. However, the analytic form of the eigenvalues for this type of matrices is only known for heptadiagonal ones (see, Solary, 2013). We generalize this link between the eigenstructure and the associated harmonics by the use of circulant matrices.

In this section, we propose an automatic version of SSA based on circulant matrices. First, we deal with the stationary case and later on we will extend our proposal to the nonstationary case.

## 3.1 Stationary case

In this subsection we propose to apply SSA to an alternative matrix of second moments that is circulant. In this case, we have closed form eigenvalues-eigenvectors that are linked to the desirable specific frequencies. We show the asymptotic equivalence between the traditional Toeplitz matrices used in SSA and our proposed circulant matrices. We also propose a more friendly and very easy to estimate approach to the elements of the circulant matrix. Based on all the previous results we propose a new alghorithm that we name Circulant SSA (CSSA).

Toeplitz matrices appear when considering the population second order moments of the trajectory matrix. Let $\{x_t\}$ be an infinite, zero mean stationary time series whose autocovariances are given by $\gamma_m = E(x_t x_{t-m})$ $m = 0, 1, ...$ and its spectral density function, a real $2\pi$-periodic, continuous function, denoted by $f$. Let

$$\mathbf{\Gamma}_L(f) = \begin{pmatrix} \gamma_0 & \gamma_1 & \gamma_2 & \cdots & \gamma_{L-1} \\ \gamma_1 & \gamma_0 & \gamma_1 & \cdots & \gamma_{L-2} \\ \vdots & \vdots & \vdots & \vdots & \vdots \\ \gamma_{L-1} & \gamma_{L-2} & \gamma_{L-3} & \cdots & \gamma_0 \end{pmatrix} \tag{2}$$

be the $L \times L$ matrix that collects the second moments. Notice that $\mathbf{\Gamma}_L(f)$ is a symmetric Toeplitz matrix that depends on the spectral density $f$ through the covariances $\gamma_m$. Recall that $\gamma_m = \int_0^1 f(w) \exp(i2\pi m w) dw$ for any integer $m$ where $w$ is the frequency in cycles per unit of time.

Analytic expressions for the eigenvalues of Toeplitz matrices are only known up to heptadiagonal matrices. To be able to have closed solutions of the eigenvalues and eigenvectors for any dimension, we use a special case of Toeplitz matrices that are the circulant ones. In a circulant matrix every row is a right cyclic shift of the row above as follows:

$$\mathbf{C}_L(f) = \begin{pmatrix} c_0 & c_1 & c_2 & ... & c_{L-1} \\ c_{L-1} & c_0 & c_1 & ... & c_{L-2} \\ \vdots & \vdots & \vdots & \vdots & \vdots \\ c_1 & c_2 & c_3 & ... & c_0 \end{pmatrix}.$$

Following Lancaster (1969), the $k$-th eigenvalue of the $L \times L$ circulant matrix $\mathbf{C}_L(f)$ is given by

$$\lambda_{L,k} = \sum_{m=0}^{L-1} c_m \exp\left(i2\pi m \frac{k-1}{L}\right)$$

for $k = 1, ..., L$ with associated eigenvector

$$\mathbf{u}_k = L^{-1/2}(u_{k,1,}..., u_{k,L})' \tag{3}$$

where $u_{k,j} = \exp\left(-i2\pi(j-1)\frac{k-1}{L}\right)$.

In particular, if we consider the circulant matrix of order $L \times L$ with elements $c_m$ defined as:

$$c_m = \frac{1}{L}\sum_{j=0}^{L-1} f\left(\frac{j}{L}\right)\exp\left(i2\pi m\frac{j}{L}\right), \qquad m = 0, 1, ..., L-1, \tag{4}$$

we have two interesting results. First, the eigenvalues of this circulant matrix coincide with the spectral density evaluated at points $w = \frac{k-1}{L}$,

$$\lambda_{L,k} = f\left(\frac{k-1}{L}\right); \tag{5}$$

and second, the matrices $\mathbf{\Gamma}_L(f)$ and $\mathbf{C}_L(f)$ are asymptotically equivalent as $L \to \infty$, $\mathbf{\Gamma}_L(f) \sim \mathbf{C}_L(f)$, in the sense that both matrices have bounded eigenvalues and $\lim_{L\to\infty} \frac{\|\mathbf{\Gamma}_L(f)-\mathbf{C}_L(f)\|_F}{\sqrt{L}} = 0$, where $\|\cdot\|_F$ is the Frobenius norm, as Gray (1972; lemma 4.1) shows. Moreover, the eigenvalues of both matrices $\mathbf{\Gamma}_L(f)$ and $\mathbf{C}_L(f)$ are asymptotically equally distributed in the sense of Weyl[1] as a consequence of the fundamental theorem of Szegö (Grenander and Szegö, 1958) as Trench (2003) shows.

To obtain a more operational version of the procedure, we consider a new circulant matrix $\widetilde{\mathbf{C}}_L(f)$ whose elements $\widetilde{c}_m$ are given by

$$\widetilde{c}_m = \frac{L-m}{L}\gamma_m + \frac{m}{L}\gamma_{L-m}, \qquad m = 0, 1, ..., L-1. \tag{6}$$

In this case, Pearl (1973) shows that $\mathbf{\Gamma}_L(f)$ is asymptotically equivalent to $\widetilde{\mathbf{C}}_L(f)$. By the transitivity property, the three matrices $\mathbf{\Gamma}_L(f)$, $\widetilde{\mathbf{C}}_L(f)$ and $\mathbf{C}_L(f)$ are asymptotically equivalent.

Therefore, our proposal will consist on using these closed forms of the eigenvalues and eigenvectors to associate the SSA elementary components to a particular frequency before extracting them. Moreover, with this approach the spectral density is easily evaluated at frequencies $\frac{k-1}{L}$ by the eigenvalues of the $\widetilde{\mathbf{C}}_L(f)$ matrix.

Finally, to deal with observed data we have to work with estimated, rather than population, quantities. So, we substitute the population autocovariances $\{\gamma_m\}_{m=0}^{L-1}$, by the sample second moments $\{s_m\}_{m=0}^{L-1}$ where $s_m, m = 0, ..., L-1$ is defined as

$$s_m = \frac{1}{T-m}\sum_{t=1}^{T-m} x_t x_{t-m}.$$

[1] Weyl defines two sets of bounded real numbers $\{a_{n,k}\}_{k=1}^{n}$ and $\{b_{n,k}\}_{k=1}^{n}$as asymptotically equally distributed if for a given continuous function $F$ on the interval $[-K, K]$, it holds that $\lim_{n\to\infty} \frac{\sum_{k=1}^{n}\left(F(a_{n,k})-F(b_{n,k})\right)}{n} = 0$.

Since the sample autocovariances converge in probability to the population autocovariances, we define $S_C$ with elements given by

$$\widehat{c}_m = \frac{L-m}{L} s_m + \frac{m}{L} s_{L-m}, \qquad m = 0, 1, ..., L-1. \tag{7}$$

In what follows, we describe our new proposed algorithm, named Circulant SSA. Given the time series data $\{x_t\}_{t=1}^T$:

**1st step: Embedding.** This step is as before.

**2nd step: Decomposition.** Compute the circulant matrix $S_C$ whose elements are given in (7). Find the eigenvalues $\widehat{\lambda}_k$ of $S_C$ and based on (5), associate the $k$-th eigenvalue to the frequency $w = \frac{k-1}{L}, k = 1, ..., L$.

**3rd step: Grouping.** Given the symmetry of the spectral density, we have that $\widehat{\lambda}_k = \widehat{\lambda}_{L+2-k}$. Their corresponding eigenvectors given by (3) are complex, therefore, they are conjugated complex by pairs, $\mathbf{u}_k = \overline{\mathbf{u}}_{L+2-k}$ where $\overline{\mathbf{v}}$ indicates the complex conjugate of a vector $\mathbf{v}$, and $\mathbf{u}_k^*\mathbf{X}$ and $\mathbf{u}_{L+2-k}^*\mathbf{X}$ correspond to the same harmonic period, where $\mathbf{v}^*$ denotes the transpose conjugate of $\mathbf{u}_k$ . We proceed as follows to transform them in pairs of real eigenvectors in order to compute the associated components.

To form the elementary matrices we first form the groups of 2 elements $B_k = \{k, L+2-k\}$ for $k = 2, ..., M$ with $B_1 = \{1\}$ and $B_{\frac{L}{2}+1} = \left\{\frac{L}{2}+1\right\}$ if $L$ is even. Second, we compute the elementary matrix by frequency $\mathbf{X}_{B_k}$ as the sum of the two elementary matrices $\mathbf{X}_k$ and $\mathbf{X}_{L+2-k}$, associated to eigenvalues $\widehat{\lambda}_k$ and $\widehat{\lambda}_{L+2-k}$ and frequency $\frac{k-1}{L}$,

$$\begin{aligned}
\mathbf{X}_{B_k} &= \mathbf{X}_k + \mathbf{X}_{L+2-k} \\
&= \mathbf{u}_k\mathbf{u}_k^*\mathbf{X} + \mathbf{u}_{L+2-k}\mathbf{u}_{L+2-k}^*\mathbf{X} \\
&= (\mathbf{u}_k\mathbf{u}_k^* + \overline{\mathbf{u}}_k\overline{\mathbf{u}}_k^*)\mathbf{X} \\
&= 2(R_{\mathbf{u}_k}R_{\mathbf{u}_k}^{'} + I_{\mathbf{u}_k}I_{\mathbf{u}_k}^{'})\mathbf{X}
\end{aligned}$$

where the prime denotes transpose, $R_{\mathbf{u}_k}$ denotes the real part of $\mathbf{u}_k$ and $I_{\mathbf{u}_k}$ its imaginary part. In this way, all the matrices $\mathbf{X}_k, k = 1, ..., L$, are real.

**4th step: Reconstruction**. As before.

Notice that the elementary reconstructed series by frequency can be automatically assigned to a component according to the goal of our analysis.

### 3.2 Nonstationary case

In economics, many time series are nonstationary. That is to say, the autoregressive polynomial has unit roots. This has important consequences in our analysis and we have to

show that Circulant SSA can be applied to nonstationary time series. The next theorem, a generalization of the analogous given by Gray (1974), provides the theoretical background needed to apply Circulant SSA to nonstationary time series.

**Theorem 1** *Let $\mathbf{T}_L(s)$ be a sequence of Toeplitz matrices with $s(w)$ a real, continuous and $2\pi$-periodic, such that $s(w) \geq 0$, where the equality is reached in a finite number of points $H = \{w_i^0, i = 1, ..., l\}$. Given a finite $\delta$, consider the disjoint sets*

$$\Omega_i = \left\{ w \in \left[ w_i^0 - a_i, w_i^0 + b_i \right] | s(w) \leq \frac{1}{\delta} \right\}, a_i, b_i \in \mathbb{R}^+, i = 1, ..., l$$

*and let $g(w)$ be a function defined as*

$$g(w) = \left\{ \begin{array}{ll} f(w) = \frac{1}{s(w)} \text{ if } w \notin \cup_{i=1}^{l} \Omega_i \\ h_i(w) \qquad \text{if } w \in \Omega_i \end{array} \right\}$$

*where $h_i(w)$ is any real valued bounded function continuous in $\Omega_i$. Let $M_{h_i} = ess\ sup\ h_i < \infty$ and $m_{h_i} = ess\ inf\ h_i = h_i\left(w_i^0 - a_i\right) = h_i\left(w_i^0 + b_i\right) = \delta$.*

*Let $\rho_{L,k}, k = 1, ..., L$, be the eigenvalues of $(\mathbf{T}_L(s))^{-1}$ sorted in decreasing order and let $F(x)$ be a continuos function in $\left[\frac{1}{M_s}, \max_i M_{h_i}\right]$ with $M_s = ess\ sup\ s$, then*

$$\lim_{L \to \infty} \frac{1}{L} \sum_{k=1}^{L} F(\min(\rho_{L,k}, \max(\widetilde{g}_k, \delta))) = \int_0^1 F(g(w)) dw, \tag{8}$$

*where $\widetilde{g}_k$ are the values of $g(\frac{k-1}{L})$ sorted in descending order.*

**Proof**: The proof is given in the Appendix.

In a similar way to Gray (1974), the theorem states that the sequence of eigenvalues of the sequence of matrices $(\mathbf{T}_L(s))^{-1}$ are asymptotically distributed (in the sense of Weyl) as the eigenvalues of the sequence of matrices $\mathbf{T}_L(g)$ up to a finite value $\delta$ as $L$ tends to infinity. Moreover, the matrices $\mathbf{T}_L(g) \sim \mathbf{C}_L(g)$ and by Szegö's theorem, the eigenvalues of the sequence of matrices $\mathbf{T}_L(g)$ are asymptotically distributed as the eigenvalues of the sequence of matrices $\mathbf{C}_L(g)$ up to a finite value $\delta$ as $L$ tends to infinity.

As a result, for a nonstationary series, the union of the estimation of the spectral density in a point of discontinuity with the estimations in the adjoint frequencies through segments is an easy way of building the functions $h_i$. If all the functions $h_i$ are constant and equal to a particular value $\delta$ finite , we have the particular case proved in Gray (1974). Therefore, the generalization to functions $h_i$ allows a better approximation of the spectral density when we increase the window length.

# 4 Separability of SSA

Separability of the elementary series as well as those grouped by frequencies is an assumption of SSA and should also be a characteristic of the estimated components. This characteristic is important since many signal extraction procedures assume zero correlation between their underlying components, whereas the estimated signals can be quite correlated. As Golyandina et al. (2001) point out the SSA decomposition can be successful only if the resulting additive components of the series are quite separable from each other. In this section, we first introduce the basic notions of separability and how it is measured. Afterwards, we show that Circulant SSA produces component series that are highly separable outperforming alternative algorithms.

For a fixed window length $L$, given two series $\left\{x_t^{(1)}\right\}$ and $\left\{x_t^{(2)}\right\}$ extracted from the series $\{x_t\}$, we say that they are weakly separable if both their column as well as row spaces are orthogonal, that is $\mathbf{X}^{(1)}\left(\mathbf{X}^{(2)}\right)' = \mathbf{0}_{L\times L}$ and $\left(\mathbf{X}^{(1)}\right)'\mathbf{X}^{(2)} = \mathbf{0}_{N\times N}$. Furthermore, we say that two series $\left\{x_t^{(1)}\right\}$ and $\left\{x_t^{(2)}\right\}$ are strongly separable if they are weakly separable and the two sets of singular values of the trajectory matrices $\mathbf{X}^{(1)}$ and $\mathbf{X}^{(2)}$ are disjoint. When the trajectory matrix of the original time series has not multiple singular values or, equivalently, each elementary reconstructed series belongs to a different harmonic, strong separability is guaranteed according to the previous definition.

Usually, separability is measured in terms of **w**-correlation (see, for instance, Golyandina et al., 2001, and Golyandina and Zhigljavsky, 2013), that it is given by

$$\rho_{12}^{w} = \frac{\left\langle \mathbf{x}^{(1)}, \mathbf{x}^{(2)} \right\rangle_w}{\left\|\mathbf{x}^{(1)}\right\|_w \left\|\mathbf{x}^{(1)}\right\|_w},$$

where $\left\langle \mathbf{x}^{(1)}, \mathbf{x}^{(2)} \right\rangle_w = (\mathbf{x}^{(1)})'\mathbf{W}\mathbf{x}^{(2)}$ is the so called w-inner product and $\left\|\mathbf{x}^{(1)}\right\|_w = \sqrt{\left\langle \mathbf{x}^{(1)}, \mathbf{x}^{(1)} \right\rangle_w}$ and $\mathbf{W} = diag(1, 2, ..., \overbrace{L, ..., L}^{T-2(L-1) \text{ times}}, ..., 2, 1)$. Note that the window length $L$ enters the definition of **w**-correlation. We are interested on producing components with **w**-correlation (ideally) zero because, in this case, we can conclude that the component series are **w**-orthogonal, i. e. $\left\langle \mathbf{x}^{(1)}, \mathbf{x}^{(2)} \right\rangle_w = 0$ and separable (see, Golyandina et al. 2001). To quickly check how separable are the component series when performing SSA, we plot the matrix of the absolute values of the **w**-correlations for all the component series, coloring in white the absence of **w**-correlation, in black **w**-correlations in absolute value equal to 1 and in a scale of grey colors the remaining intermediate values.

To show that Circulant SSA produces components that are strongly separable, first notice that the real eigenvectors $\sqrt{2}R_{\mathbf{u}_k}$ and $\sqrt{2}I_{\mathbf{u}_k}$ (linked to eigenvalues $\lambda_k$ and $\lambda_{L+2-k}$, respectively, $\lambda_k = \lambda_{L+2-k}$) are orthogonal and have information associated only to frequency $\frac{k-1}{L}$ . Those are the only eigenvectors that have information related to this frequency. As eigenvectors can be considered filters, Kume (2013), these pair of eigenvectors extract elementary series linked to the same frequency without mixing harmonics of other frequencies. As a result, the two elementary series, when reconstructed in step 4, have spectral correlation close to 1 between them and close to zero with the remaining ones. Taking into account the pairs of reconstructed series per frequency, any grouping of the reconstructed series results in disjoint sets from the point of view of the frequency. Then, Circulant SSA produce components that are approximately strongly separable. In this case, the graph of the **w**-correlation matrix is black color in the main diagonal and white elsewhere as in the ideal case.

As we shall see in the simulation and in the empirical application, CSSA produces components that are more separable than previous alternatives os SSA, Basic and Toeplitz.

# 5 Simulations

In this section we compare the performance of our new proposal, Circulant SSA, with the competing SSA algorithms, i.e. Basic SSA and Toeplitz SSA for a linear as well as nonlinear time series model. We focus on two main aspects: reliability of the estimated components in finite samples and separability.

## 5.1 Linear time series

The first model is a basic structural time series model

$$x_t = T_t + c_t + s_t + e_t \tag{9}$$

where $T_t$ is the trend component, $c_t$ is the cycle, $s_t$ is the seasonal component and $e_t$ is the irregular component. We assume an integrated random walk for the trend (see Young 1984) given by

$$\begin{aligned} T_t &= T_{t-1} + \beta_{t-1} \\ \beta_t &= \beta_{t-1} + \eta_t \end{aligned} \tag{10}$$

with $\eta_t \sim N(0, \sigma_\eta^2)$. The cyclical and seasonal components are specified according to Durbin and Koopman (2012), where the cycle is given by the first component of the bivariate VAR(1)

$$\begin{pmatrix} c_t \\ \widetilde{c}_t \end{pmatrix} = \rho_c \begin{pmatrix} \cos(2\pi w_c) & \sin(2\pi w_c) \\ -\sin(2\pi w_c) & \cos(2\pi w_c) \end{pmatrix} \begin{pmatrix} c_{t-1} \\ \widetilde{c}_{t-1} \end{pmatrix} + \begin{pmatrix} \varepsilon_t \\ \widetilde{\varepsilon}_t \end{pmatrix} \tag{11}$$

with $\begin{pmatrix} \varepsilon_t \\ \widetilde{\varepsilon}_t \end{pmatrix} \sim N(\mathbf{0}, \sigma_\varepsilon^2 I)$ and $\frac{1}{w_c}$ the period with $w_c \in [0, 1]$. The seasonal component is given by

$$s_t = \sum_{j=1}^{[s/2]} a_{j,t} \cos(2\pi w_j t) + b_{j,t} \cos(2\pi w_j t) \tag{12}$$

with $w_j = \frac{j}{s}, j = 1, ..., [s/2]$ and $s$ the seasonal period, where $[\cdot]$ is the integer part and $a_{j,t}$ and $b_{j,t}$ are two independent random walks with noise variances equal to $\sigma_j^2$. Finally, the irregular component is white noise with variance $\sigma_e^2$. All the components are independent of each other. We set $\rho_c = 1$, so the trend, cycle and seasonal components have a unit root. We consider that the series are monthly with $s = 12$ and cyclical period equal to $\frac{1}{w_c} = 48$ months. The sample size is $T = 193$ and the noise variances of the different components are given by $\sigma_\eta^2 = 0.0006^2$, $\sigma_j^2 = 0.004^2$, $\sigma_\varepsilon^2 = 0.008^2$ and $\sigma_e^2 = 0.06^2$. We choose as window length $L = 48$ following Golyandina and Zhigljavsky (2013), since $L$ is multiple of the seasonal period, it is equal to the cyclical period and $T - 1$ is multiple of $L$.

The trend is related to the 0 frequency, the cycle to frequency 1/48 and the seasonal components to frequencies 1/12, 1/6, 1/3, 1/4, 5/12 and 1/2. Then, according to (5) and the symmetry of the spectral density, the trend is reconstructed with the eigentriple 1, the cyclical component with the eigentriples 2 and 48, and the seasonal components with the eigentriples 5, 9, 13, 17, 21, 25, 29, 33, 37, 41 and 45. For example, for the frequency $w = \frac{1}{12}$, we have that $\frac{k-1}{L} = \frac{1}{12}$, and therefore, we sum the elementary components $k = \frac{48}{12} + 1 = 5$ and $L + 2 - k = 48 + 2 - 5 = 45$.

If the procedure for signal extraction works well, the simulated component $y_t$ ($y_t$ can be the trend, cycle or seasonal component) could be written as

$$y_t = \widehat{y}_t + u_t$$

where $u_t$ is the noise and $\widehat{y}_t$ is the extracted signal. Then, in the regression

$$y_t = a + b\widehat{y}_t + e_t \tag{13}$$

$a = 0$ (unbiasedness) and $b = 1$ (the scale is not changed). We simulate 1000 times the model and perform signal extraction with Circulant SSA. Table 1 shows the percentiles of the empirical distribution of the estimated coefficients of the regression in (13). The last three rows of the table show the inverse of the signal to noise ratio

$$SNR^{-1} = \frac{\sigma_u^2}{\sigma_s^2}$$

where $\sigma_u^2$ is the variance of the noise $u_t = y_t - \widehat{y}_t$ and $\sigma_s^2$ is the variance of the estimated signal $\widehat{y}_t$. A value close to zero indicates that the explanatory power of the noise is very small compared to that of the signal and it is an indication of a good approximation. Table 1 shows that the median of the estimated intercept and is almost zero for the three estimated components (cycle, seasonal component and trend). The median for the scale parameter $b$ is almost one for the three components, but looking at the values for different quantiles, the empirical distribution for the estimated $b$ associated to the cycle indicates a larger dispersion.

TABLE 1 SHOULD BE INSERTED AROUND HERE

The estimated residuals from equation (9) are given by $\widehat{e}_t = x_t - \widehat{T}_t - \widehat{c}_t - \widehat{s}_t$ and should be white noise. In order to check this, we fit an AR(1) to $\widehat{e}_t$. Table 2 shows the quantiles of the empirical distribution of the mean, standard error and autoregressive coefficient of the residuals of the 1000 replications. The median of the mean and autoregressive coefficient are close to zero. The median of the standard deviation is 0.0529 (the value used for the simulations was 0.06).

TABLE 2 SHOULD BE INSERTED AROUND HERE

The results from the simulations seem very good. In order to compare Circulant SSA with alternative algorithms as Basic and Toeplitz SSA, we describe in more detail the simulation corresponding to the replication number 500. With Circulant SSA, we know in advance the eigentriples corresponding to each component (trend, cycle and seasonal component). For Basic and Toeplitz SSA, we associate the eigentriples to each component (trend, cycle or seasonal component) afterwards. In this particular case, for Basic SSA, we associate the eigentriple 1 with the trend, eigentriples 2 and 3 with the cycle and eigentriples 4 to 14 with the seasonal component. For Toeplitz SSA, the trend is reconstructed with the eigentriple 1, the cycle with eigentriples 2 and 3 and the seasonal component with the eigentriples 5 to 11 and 14 to 18. We also compute the statistics associated to the error

term of the estimated components. In Table 3 we present the summary statistics for the error term as well as the inverse of the $SNR$.

TABLE 3 SHOULD BE INSERTED AROUND HERE

Although the summary statistics from Table 3 seem to show that the three algorithms (Circulant, Basic and Toeplitz SSA) produce similar results, notice that Circulant SSA produces components with smaller $SNR^{-1}$.

Regarding separability, Figure 1 plots the **w**-correlation matrices for the components extracted with the three algorithms. Notice that Circulant SSA produces matrices that are closer to diagonality than the other two alternatives where we can see different degrees of grey in the off-diagonal cells. Therefore, as it was expected, Circulant SSA recovers components that are more separable than the two alternative versions of SSA, Basic and Toeplitz.

FIGURE 1 SHOULD BE INSERTED AROUND HERE

### 5.2 Non-linear time series

For the case of non-linear time series, we borrow the model from Durbin and Koopman (2012) for UK travellers given by

$$x_t = T_t + c_t + \exp(a_0 + a_1 T_t)\gamma_t + \varepsilon_t$$

where $T_t$ is the trend, $c_t$ is the cycle and $\gamma_t$ is the seasonal component specified as in (10), (11) and (12), respectively. The parameters $a_0$ and $a_1$ are unknown fixed coefficients. Coefficient $a_0$ scales the seasonal component. The sign of the coefficient $a_1$ determines whether the seasonal variation increases or decreases when a positive change in the trend occurs. The overall time varying amplitude of the seasonal component is determined by the combination $a_0 + a_1\mu_t$.

As for the linear case, we simulate the model 1000 times for series of length $T = 193$ observations. We set $a_0$ and $a_1$ such that for each replication $0.5 \leq \exp(a_0 + a_1\mu_t) \leq 1.5$, with $a_1 > 0$. We apply Circulant SSA with a window length $L = 48$. Table 4 shows the quantiles of the empirical distribution of the estimated coefficients of the regression in (13). The last three rows of the table show the inverse of the signal to noise ratio $SNR^{-1}$.

TABLE 4 SHOULD BE INSERTED AROUND HERE

In order to check that the estimated residuals are white noise, we fit an AR(1) to $\widehat{e}_t$ as in the linear case. Table 5 shows the quantiles of the empirical distribution of the mean, standard error and autoregressive coefficient of the residuals of the 1000 replications. The median of the mean and autoregressive coefficient are close to zero. The median of the standard deviation is 0.053 (the value used for the simulations was 0.06).

TABLE 5 SHOULD BE INSERTED AROUND HERE

As in the linear case, the results from the simulations seem very good. To compare Circulant SSA with alternative algorithms as Basic and Toeplitz SSA, we describe in more detail replication number 500. Table 6 shows the summary statistics of the residuals as well as the inverses of the $SNR$ in order to check the adequacy of the three versions of SSA.

TABLE 6 SHOULD BE INSERTED AROUND HERE

Although the three algorithms seem to work quite well, Circulant SSA produces components with smaller $SNR^{-1}$. Figure 2 shows the **w**-correlation matrices for the components extracted with the three algorithms. Notice that in the nonlinear case, Circulant SSA also presents w-correlation matrices that are closer to the diagonality than the other two alternatives where we can see different degrees of grey in the off-diagonal cells. Again, Circulant SSA recovers components that are more separable than the two alternative versions of SSA, Basic and Toeplitz.

FIGURE 2 SHOULD BE INSERTED AROUND HERE

# 6 Application

We consider monthly series of Industrial Production (IP), index 2010=100, of six countries: France, Germany, Italy, UK, Japan and USA. Industrial Production is widely followed since it is pointed out in the definition of a recession by the National Bureau of Economic Research (NBER), `http://www.nber.org/cycles/recessions.html`, as one of the four monthly indicators series to check in the analysis of the business cycle. The sample covers from January 1970 to September 2014, so the sample size $T = 537$. The data source is the IMF database. As it can be seen in Figure 3, these indicators show different trend, seasonality and cyclical behavior, and our goal is to extract these components and discuss about the results.

FIGURE 3 SHOULD BE INSERTED AROUND HERE

The first step is to establish the window length. Due to the monthly periodicity and seasonality, we select a window length multiple of 12. Assuming that the period of the cycle in these series goes from 1 year and a half to 8 years, we choose a window length multiple of 8×12=96 months. From the two available options, 96 and 192 months, we select the second one since it is larger according to the asymptotic results provided in Section 3.

We apply Circulant SSA, and associate the trend to the frequencies $w = 0$ and $w = 1/192$ (as they correspond to periods of infinite and a long cycle of 16 years respectively). According to (5) and the symmetry of the spectral density, the trend is reconstructed with the eigentriples 1, 2 and 192 and with the elementary groups by frequencies $B_1$ and $B_2$ respectively. According to the assumption that the period for the cycle goes from 1.5 to 8 years, this component is associated to the frequencies $w = 1/96, 1/64, 1/48, 5/192, 1/32, 7/192, 1/24, 3/64, 5/96$ and the cycle signal is reconstructed with the eigentriples 3 to 11 and 183 to 191, with the elementary groups by frequencies from $B_3$ to $B_{11}$. Finally, the seasonal component is associated to the frequencies $w = 1/12, 1/6, 1/4, 1/3, 5/12, 1/2$ and reconstructed in a similar way with the eigentriples 17, 33, 49, 65, 81, 97, 113, 129, 145, 161 and 177 and with the elementary groups by frequencies $B_{17}, B_{33}, B_{49}, B_{65}, B_{81}$, and $B_{97}$.

Table 7 shows the contributions of the signals to the original IP variations in percentage. First, we highlight that the contribution of the irregular component (those oscillations not explained by the trend, cyclical or seasonal components) is smaller than 3.5% in all the countries. Main contributions come from the trend and seasonality, that account for more than 84% in all the countries. As expected, the contribution of the seasonal component is almost negligible in USA, and quite small in Japan and Germany, while it is very relevant in Italy and France. Finally, the cycle contributes in a range between 7.8% in Italy to 13.8% in Japan.

TABLE 7 SHOULD BE INSERTED AROUND HERE

Figure 3 shows the estimated trends for every country. The trend is a smooth component that has shown a decreasing evolution since the last decade for France, Italy and UK as a consequence of the last economic crisis. On the contrary, in Germnay and US, the trend shows an upward evolution in all the sample period.

Figure 4 shows the cyclical component where the shaded areas correspond to recessions as dated by the OECD. We can see that the extracted cycle reflects quite well the business

cycle for all countries.

FIGURES 4 AND 5 SHOULD BE INSERTED AROUND HERE

Figure 5 shows the matrices of **w**-correlations and it can be seen that, as expected, Circulant SSA produces components that are strongly separable. Separability results is a very desirable feature in the construction of seasonal adjusted time series, that is the absence of any remaining seasonality. To check the quality of seasonal adjustment by Circulant SSA, we have applied the *combined test for seasonality* (Lothian, 1978) used in X12-ARIMA. We found that there were no signs of any remaining seasonality in any of the seasonal adjusted time series for the different countries[2].

# 7 Conclusions

SSA is a nonparametric technique to extract the unobserved components present in a time series. Up to now, the intervention of the analyst was needed to identify the frequencies associated to each component. In this paper, we propose a new version of SSA, Circulant SSA, that does not need the intervention of the analyst. It relies on the asymptotic equivalence between Toeplitz and circulant matrices of second order moments of time series. The properties of circulant matrices allow to estimate the spectral density of a time series at certain frequencies through the eigenvalues. We can also identify automatically and a priori the frequencies associated to those eigenvalues. In this way, results are obtained very fast and with no subjective intervention from the analyst.

We also extend the algorithm to the nonstationary case providing a generalization of Gray's theorem (1974).

The eigenvectors obtained from the diagonalization of the circulant matrix associated to second moments of the original series are real and form an orthonormal basis in the column space of the trajectory matrix. As a result, we can guarantee that all the elemental components are real. Additionally, they are strongly separable, so it is easy to group the elemental series to obtain the different signals (trend, cycle, seasonality...). We have compared our version of SSA to two already available ones (Basic and Toeplitz SSA) and although the final results are quite similar, Circulant SSA is faster, automatic and produces more separable components.

[2]Results are available from the authors upon request.

The properties of Circulant SSA have been checked through a set of simulations for linear and nonlinear time series models as well as through the empirical application where we showed that Circulant SSA produced deseasonalize series clean of any seasonality. The cycle was also very useful to study the business cycle.

# 8 Appendix

**Proof of Theorem 1:** As defined, the function $g(w)$ is real, continuous and $2\pi$-periodic. Its image is $\left[\frac{1}{M_s}, \max_i M_{h_i}\right]$ being different from zero in the whole interval. Then, by the properties of the inverse of Toeplitz matrices $\left(\mathbf{T}_L(g^{-1})\right)^{-1} \sim \mathbf{T}_L(g)$. Moreover, if $F(x)$ is continuos in $\left[\frac{1}{M_s}, \max_i M_{h_i}\right]$, then $F(\frac{1}{x})$ is continuos in $\left[\frac{1}{\max_i M_{h_i}}, M_s\right]$. Given that Gutiérrez and Gutiérrez (2012) relax the assumption of $g(w)$ being a Wiener's class function to a continuous and $2\pi$-periodic function, Szegö's Theorem leads to (8). ■

# References


[1] Alexandrov, T. and Golyandina, N. (2004). The automatic extraction of time series trend and periodical components with the help of the Caterpillar-SSA approach. Exponenta Pro, 3-4, 54-61.

[2] Alexandrov, T. and Golyandina, N. (2005). Automatic extraction and forecast of time series cyclic components within the framework of SSA. Proceedings of the Fifth Workshop on Simulation, 45–50.

[3] Alonso, F.J. and Salgado, D.R. (2008). Analysis of the structure of vibration signals for tool wear detection. Mechanical Systems and Signal Processing, 22 (3), 735-748.

[4] Arteche, J., and García-Enríquez, J. (2016). Singular Spectrum Analysis for signal extraction in Stochastic Volatility models. Econometrics and Statistics.

[5] Bilancia, M. and Campobasso, F. (2010). Airborne particulate matter and adverse health events: robust estimation of timescale effects. In Classification as a Tool for Research, 481-489. Springer Berlin Heidelberg.

[6] Bozzo, E., Carniel, R. and Fasino, D. (2010). Relationship between Singular Spectrum Analysis and Fourier analysis: Theory and application to the monitoring of volcanic activity. Computers and Mathematics with Applications, 60, 812-820.

[7] Broomhead, D. and King, G. (1986a). Extracting qualitative dynamics from experimental data. Physica D, 20, 217–236.

[8] Broomhead, D. and King, G. (1986b). On the qualitative analysis of experimental dynamical systems. In Nonlinear Phenomena and Chaos, 113–144. A. Hilger ed., Bristol.

[9] Danilov, D. and Zhigljavsky, A. (editors) (1997). Principal components of time series: the "Caterpillar" method. Saint Petersburg Press, Saint Petersburg (in Russian).

[10] de Carvalho, M., Rodrigues, P. C., & Rua, A. (2012). Tracking the US business cycle with a singular spectrum analysis. Economics Letters, 114(1), 32-35.

[11] de Carvalho, M., and Rua, A. (2017). Real-time nowcasting the US output gap: Singular spectrum analysis at work. International Journal of Forecasting. 33 (1), 185–198.

[12] Durbin, J. and Koopman, S.J. (2012). Time Series Analysis by State Space Methods. Second edition. Oxford University Press.

[13] Elsner, J.B. and Tsonis, A.A. (1996). Singular spectrum analysis: a new tool in time series analysis. Plenum, New York.

[14] Fraedrich, K. (1986). Estimating the dimension of weather and climate attractors. Journal of the Atmospheric Sciences, 43 (5), 419–432.

[15] Ghil, M. and Mo, K. (1991). Intraseasonal oscillations in the global atmosphere. Part I and Part II, Journal of the Atmospheric Sciences, 48 (5), 752-790.

[16] Golyandina, N., Nekrutkin, V. and Zhigljavsky, A. (2001). Analysis of Time Series Structure: SSA and Related Techniques. Chapman & Hall/CRC.

[17] Golyandina, N. and Zhigljavsky, A. (2013). Singular Spectrum Analysis for Time Series. Springer.

[18] Gray, R.M. (1972). On the Asymptotic Eigenvalue Distribution of Toeplitz Matrices. IEEE Transanctions on Information Theory, 18 (6), 725–730.

[19] Gray, R.M. (1974). On Unbounded Toeplitz Matrices and Nonstationary Time Series with an Application to Information Theory. Information and Control, 24, 181–196.

[20] Grenander, U. and Szegö, G. (1958). Toeplitz Forms and Their Applications. University of California Press, Berkeley and Los Angeles.

[21] Gutiérrez-Gutiérrez, J., and Crespo, P. M. (2012). Foundations and Trends® in Communications and Information Theory. Foundations and Trends® in Communications and Information Theory, 8(3), 179-257.

[22] Hassani, H., Heravi, S., Brown, G., and Ayoubkhani, D. (2013). Forecasting before, during, and after recession with singular spectrum analysis. Journal of Applied Statistics, 40(10), 2290-2302.

[23] Hassani, H., Heravi, S., and Zhigljavsky, A. (2013). Forecasting UK industrial production with multivariate singular spectrum analysis. Journal of Forecasting, 32(5), 395-408.

[24] Hassani, H., Soofi, A. S., and Zhigljavsky, A. (2013). Predicting inflation dynamics with singular spectrum analysis. Journal of the Royal Statistical Society: Series a (Statistics in Society), 176 (3), 743-760.

[25] Hassani, H., Thomakos, D. (2010). A review on singular spectrum analysis for economic and financial time series. Statistics and its Interface, 3(3), 377-397.

[26] Kume, K. (2013). Interpretation of singular spectrum analysis as complete eigenfilter decomposition. Advances in Adaptive Data Analysis, 4 (4).

[27] Lancaster, P. (1969). Theory of Matrices. Academic Press, NY.

[28] Lothian, J. (1978). The Identification and Treatment of Moving Seasonality in the X-11 Seasonal Adjustment Method. StatCan Staff Paper STC0803E, Seasonal Adjustment and Time Series Analysis Staff, Statistics Canada, Ottawa.

[29] Pearl, J. (1973). On Coding and Filtering Stationary Signals by Discrete Fourier Transform. IEEE Trans. on Info. Theory, IT-19, 229–232.

[30] Sella, L., Vivaldo, G., Groth, A., and Ghil, M. (2016). Economic cycles and their synchronization: a comparison of cyclic modes in three European countries. Journal of Business Cycle Research, 12(1), 25-48.

[31] Silva ES, andHassani H. (2015). On the use of singular spectrum analysis for forecasting U.S. trade before, during and after the 2008 recession. International Economics.

[32] Solary, M.S. (2013). Finding eigenvalues for heptadiagonal symmetric Toeplitz matrices. Journal of Mathematical Analysis and Applications, 402, 719-730.

[33] Trench, W.F. (2003). Absolute equal distribution of the spectra of Hermitian matrices. Linear Algebra and its Applications, 366, 417-431.

[34] Vautard, R. and Ghil, M. (1989). Singular spectrum analysis in nonlinear dynamics, with applications to paleoclimatic time series. Physica D, 35, 395–424.

[35] Vautard, R., Yiou, P. and Ghil, M. (1992). Singular-spectrum analysis: A toolkit for short, noisy chaotic signal. Physica D, 58, 95–126.

[36] Young, P.C. (1984). Recursive Estimation and Time Series Analysis: An Introduction. Springer Verlag, Berlin.

# 9 Tables and Figures

| | | Quantiles | | | | |
|---|---|---|---|---|---|---|
| Statistic | Component | 5 | 25 | 50 | 75 | 95 |
| | Trend | -.058 | -.023 | -.012 | .019 | .054 |
| $a$ | Cycle | -.010 | -.004 | .000 | .005 | .011 |
| | Seasonal | -.002 | -.001 | .000 | .001 | .002 |
| | Trend | .975 | .996 | 1.004 | 1.015 | 1.062 |
| $b$ | Cycle | .854 | .957 | 1.005 | 1.046 | 1.126 |
| | Seasonal | .947 | .983 | 1.006 | 1.029 | 1.064 |
| | Trend | .001 | .002 | .005 | .021 | .169 |
| $SNR^{-1}$ | Cycle | .018 | .041 | .085 | .179 | .522 |
| | Seasonal | .035 | .052 | .070 | .092 | .139 |

**Table 1**. Statistics related to the goodness of fit of the extracted signals. The first columns are quantiles of the empirical distribution of the estimated coefficients of the regression of the generated components over the extracted ones; the last three rows show the inverse of the signal to noise ratio.

| | Quantiles | | | | |
|---|---|---|---|---|---|
| Statistic | 5 | 25 | 50 | 75 | 95 |
| Mean | -.003 | -.001 | .000 | .001 | .003 |
| S.E. | .048 | .051 | .053 | .055 | .058 |
| $\rho$ | -.173 | -.083 | -.031 | .028 | .117 |

**Table 2**. Quantiles of the empirical distribution of the statistics related to the residuals.

| | Statsitics for $\widehat{e}_t$ | | | $SNR^{-1}$ | | |
|---|---|---|---|---|---|---|
| Algorithm | Average | S.E. | $\rho$ | Trend | Cycle | Seas |
| Circulant | .004 | .053 | -.063 | .0008 | .0133 | .0586 |
| Basic | -.001 | .053 | -.073 | .0014 | .0140 | .0599 |
| Toeplitz | .001 | .054 | -.059 | .0008 | .0194 | .0651 |

**Table 3**. Summary statistics of the residuals of the model $\widehat{e}_t$ (columns 2 to 4) and inverses of the SNR (columns 5 to 7) for the replication number 500.

| | | Quantiles | | | | |
|---|---|---|---|---|---|---|
| Statistic | Component | 5 | 25 | 50 | 75 | 95 |
| | Trend | -.057 | -.020 | .000 | .021 | .058 |
| $a$ | Cycle | -.011 | -.004 | .000 | .005 | .011 |
| | Seasonal | -.002 | -.001 | .000 | .001 | .002 |
| | Trend | .971 | .995 | 1.003 | 1.014 | 1.062 |
| $b$ | Cycle | .845 | .954 | 1.002 | 1.046 | 1.138 |
| | Seasonal | .921 | .976 | 1.006 | 1.034 | 1.073 |
| | Trend | .001 | .002 | .006 | .022 | .181 |
| $SNR^{-1}$ | Cycle | .020 | .041 | .080 | .158 | .495 |
| | Seasonal | .037 | .060 | .082 | .117 | .184 |

**Table 4**. Statistics related to the goodness of fit of the extracted signals for the nonlinear model. The columns are quantiles of the empirical distribution of the estimated coefficients of the regression of the generated components over the extracted ones; the last three rows show the inverse of the signal to noise ratio.

| | Quantiles | | | | |
|---|---|---|---|---|---|
| Statistic | 5 | 25 | 50 | 75 | 95 |
| Mean | -.004 | -.001 | .000 | .001 | .003 |
| S.E. | .048 | .051 | .053 | .055 | .059 |
| $\rho$ | -.166 | -.089 | -.026 | .029 | .104 |

**Table 5**. Quantiles of the empirical distribution of the statistics related to the residuals.

| | Statsitics for $\widehat{e}_t$ | | | $SNR^{-1}$ | | |
|---|---|---|---|---|---|---|
| Algorithm | Average | S.E. | $\rho$ | Trend | Cycle | Seas |
| Circulant | -.001 | .054 | -.145 | .0020 | .0315 | .0372 |
| Basic | .002 | .054 | -.148 | .0027 | .0318 | .0403 |
| Toeplitz | .000 | .059 | -.228 | .0021 | .0433 | .0628 |

**Table 6**. Summary statistics of the residuals of the nonlinear model $\widehat{e}_t$ (columns 2 to 4) and inverses of the SNR (columns 5 to 7) for the replication number 500.

| Components | France | Germany | Italy | Japan | UK | USA |
|---|---|---|---|---|---|---|
| **Trend** | 52.1 | 77.3 | 42.7 | 79.0 | 72.0 | 87.9 |
| **Cycle** | 9.5 | 12.6 | 7.8 | 13.8 | 11.1 | 10.3 |
| **Seasonal** | 35.6 | 6.7 | 47.3 | 5.1 | 13.5 | 0.3 |
| **Irregular** | 2.8 | 3.4 | 2.2 | 2.1 | 3.4 | 1.5 |
| **Total** | 100.0 | 100.0 | 100.0 | 100.0 | 100.0 | 100.0 |

**Table 7**. Contribution (%) of the different signals to IP.

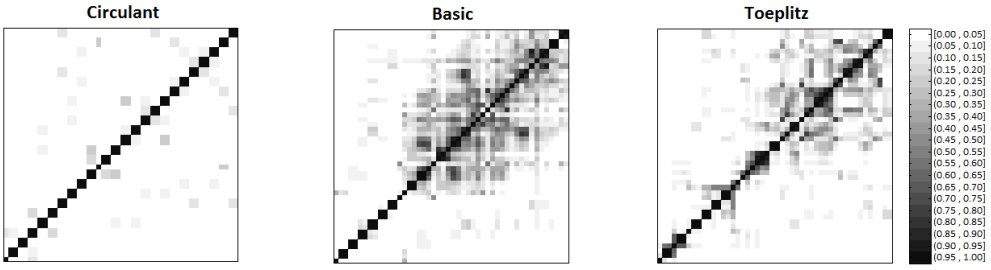


**Figure 1**: Example: w-correlations of the extracted components with Circulant, Basic and Toeplitz SSA.

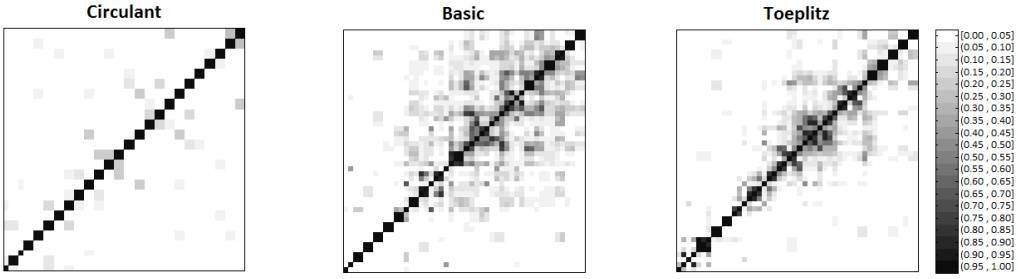


**Figure 2:** Illustrative example: w-correlations of the extracted components with Circulant, Basic and Toeplitz SSA (nonlinear case).

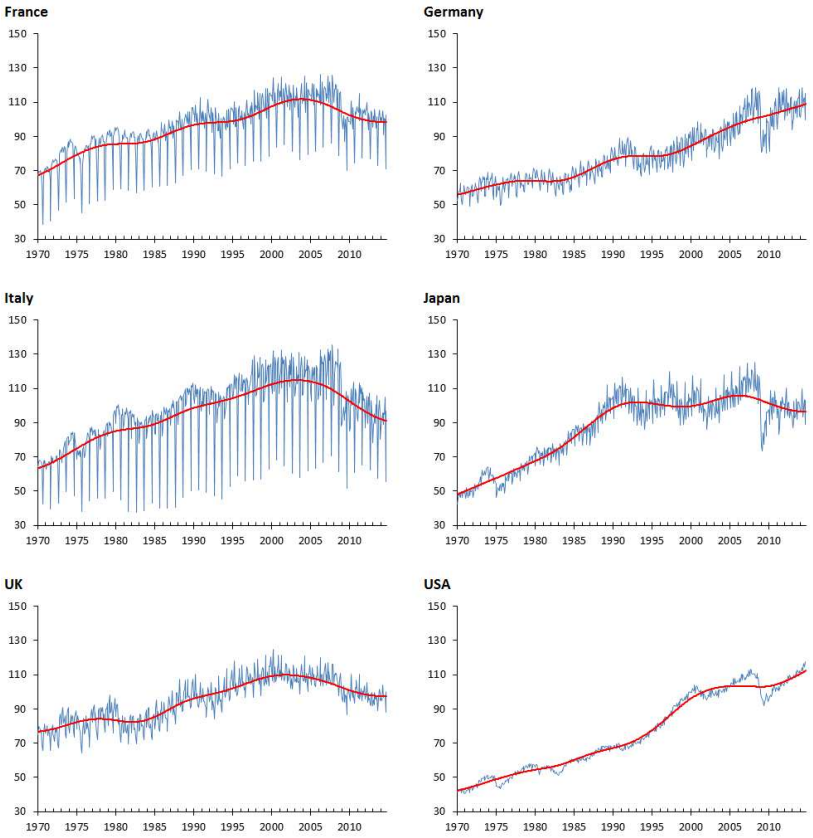


**Figure 3**: Original IP and trend for the different countries.

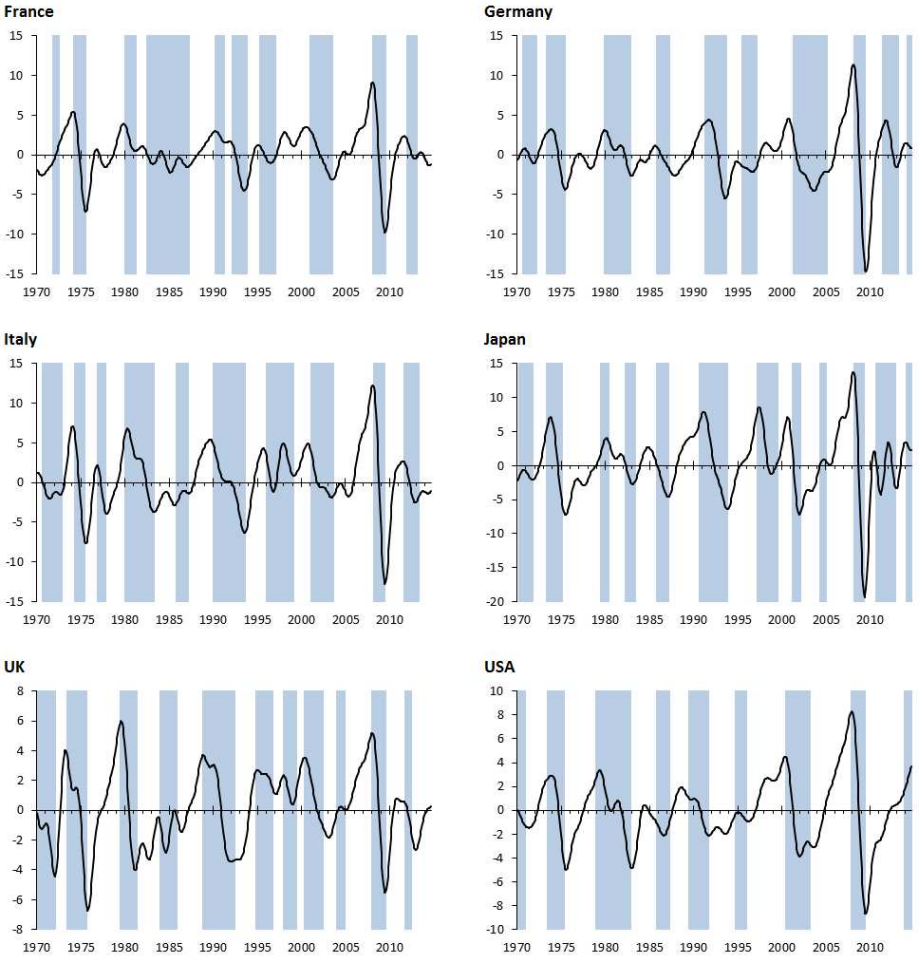


**Figure 4**. Estimated cycles and OECD announced recessions (shadowed areas).

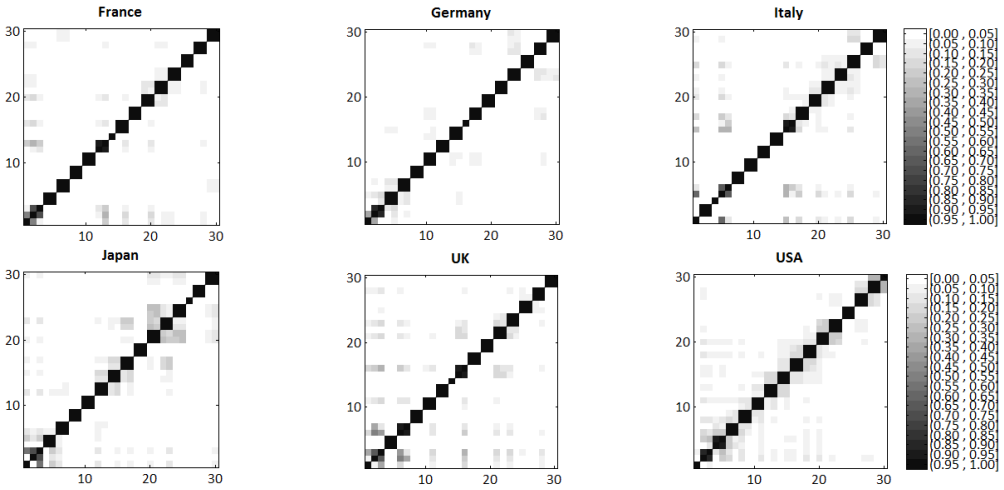


**Figure 5**. w-correlation matrix for the elementary reconstructed series for the 30 greatest eigenvalues.